Elusive Structural Changes of New Delhi Metallo-β-Lactamase Revealed by Ultraviolet Photodissociation Mass Spectrometry

M. Rachel Mehaffey[1], Yeong-Chan Ahn[2], Dann D. Rivera[2], Pei W. Thomas[2], Zishuo Cheng[3], Michael W. Crowder[3], R. F. Pratt[4], Walter Fast[2*], and Jennifer S. Brodbelt[1*]

[1]Department of Chemistry, University of Texas at Austin, Austin, TX 78712, USA
[2]Division of Chemical Biology and Medicinal Chemistry, College of Pharmacy, University of Texas at Austin, Austin, TX 78712 USA
[3]Department of Chemistry and Biochemistry, Miami University, Oxford, OH 45056 USA
[4]Department of Chemistry, Wesleyan University, Middletown, CT 06459 USA

*Corresponding authors: Jennifer S. Brodbelt, Walter Fast

Supporting Information:
Supporting information contains Figures S1-S22 which include the expressed protein sequence of NDM, structures of the covalent inhibitors, crystal structure of NDM-1 with relevant regions labelled, NDM-1 inactivation data, *p*-value plots highlighting statistical significance of measured differences, ESI-MS, HCD or UVPD MS/MS, holo ion plots, UVPD intensity plots, and difference plots or heatmaps of uninhibited NDM-1, NDM-1 bound to each of the three inhibitors, and three other clinical variants (NDM-4, NDM-6, NDM-15).

Figure S1. Sequence of (A) New Delhi Metallo-β-Lactamase-1. In subsequent figures, residues are numbered accounting for a 29 residue (no FHM) or 32 residue (with FHM) N-terminal region that is absent in the expressed sequence. Some of the proteins used in this study contain the FHM residues shaded in gold owing to differences in cleavage of the expression tag. Use of two different NDM expression and purification systems resulted in variation in the 4 and 5 positions with X4X5 = GM or GQ. The two positions mutated resulting in clinical variants are shaded: M154L (red) and A233V (green). The two reaction sites for covalent inhibitors, C208 and K211, are shaded in pink or orange, respectively. (B) Structures of covalent inhibitors of NDM-1 (**1**) pentafluorophenyl 3-mercaptopropionate, (**2**) N-(benzyloxycarbonyl)-O-[(phenoxycarbonyl)] hydroxylamine, and (**3**) ebselen. The chemical structure of the resulting modification of an amino acid side-chain is shown along with the expected mass shift.

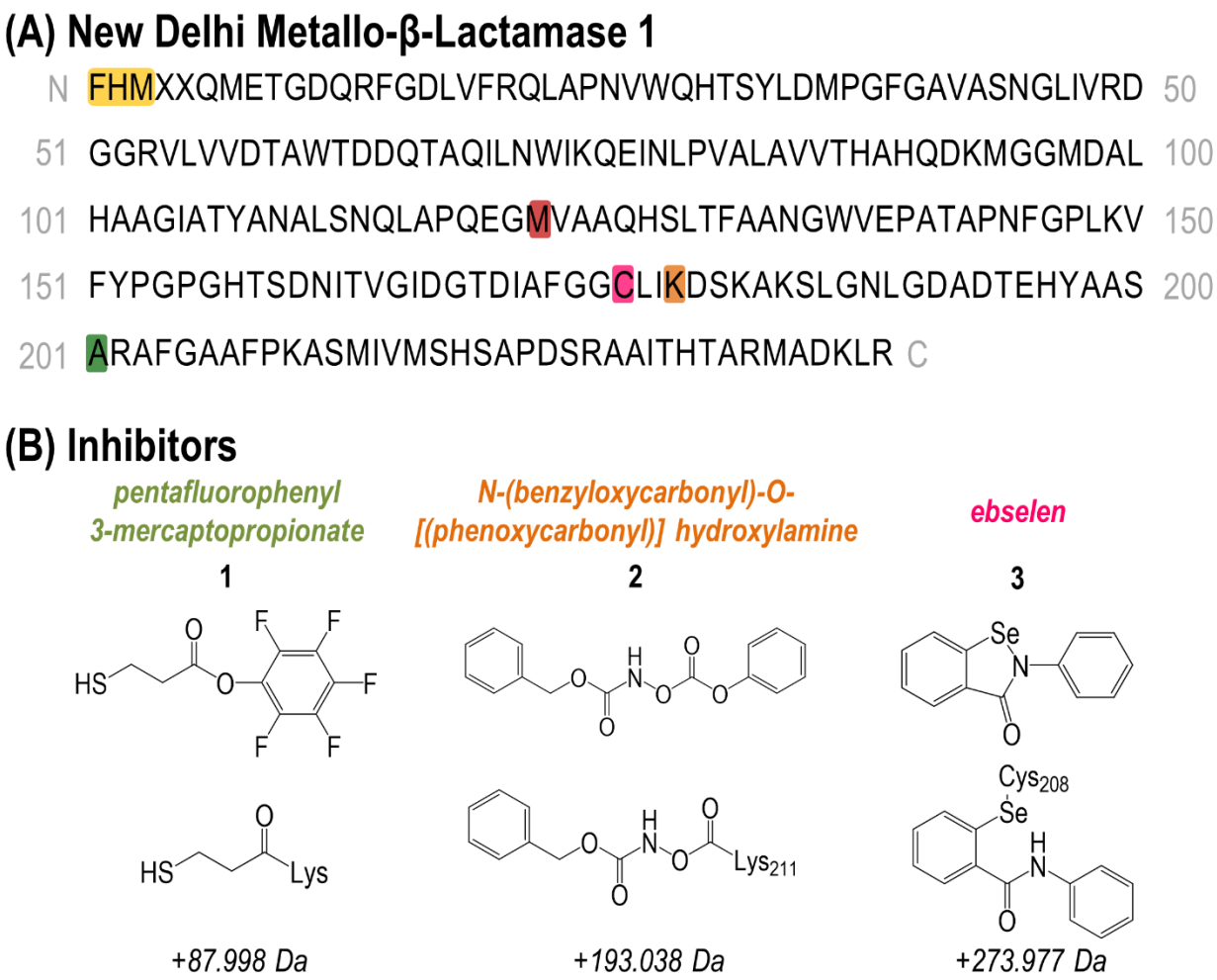

Figure S2. Log of *p*-values plotted per residue calculated from the differences for (A) NDM-1 bound to inhibitor (**2**) (Figure 3), (B) ebselen-bound NDM-1 (Figure S21), and (C) clinical variants of NDM (Figure S8). Student's *t*-test was used with pooled standard deviations to compare differences in UVPD backbone cleavage efficiencies of each inhibitor-bound protein (A, B) or clinical variant (1-3) to unreacted NDM or the reference NDM-1 sequence. Calculated *t*-values were converted to *p*-values assuming a two-tailed hypothesis. At a given residue for the inhibitor-bound or variant NDM, a *p*-value smaller than 0.01 (assuming a 99% confidence threshold represented as a black solid line) designates that the average of the triplicate measurement of UVPD intensity is statistically different from the corresponding measured average of unreacted NDM or NDM-1. (C) A histogram of calculated *p*-values in (1-3) is shown in (4) with the cumulative percentage plotted.

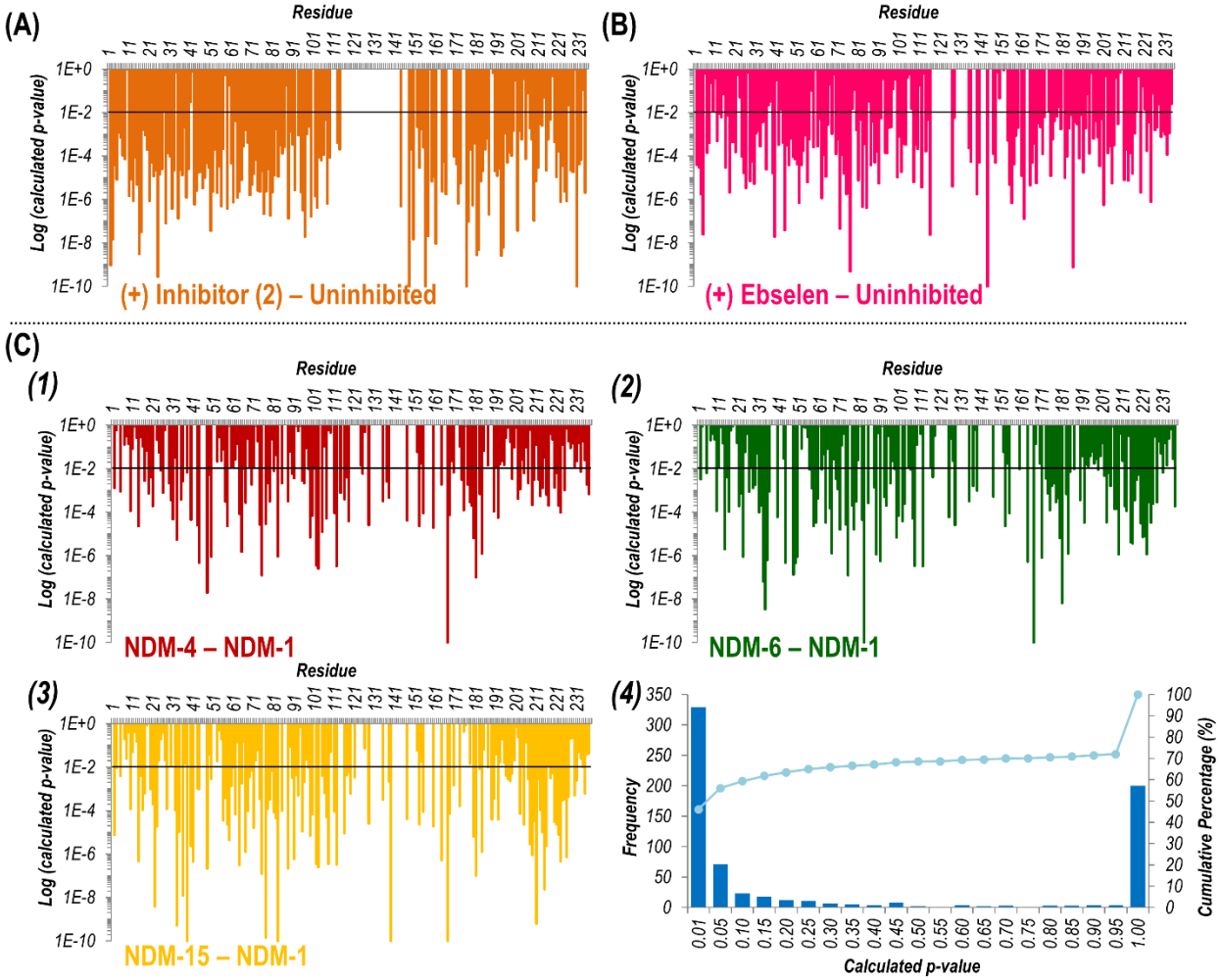

Figure S3. Crystal structure and 180° view of NDM-1 (PDB ID: 3SPU) with important loops and residues highlighted and labelled. The five active site loops (ASL) responsible for the broad substrate specificity of the protein are colored as follows: ASL1 (slate), ASL2 (turquoise), ASL3 (purple), ASL4 (olive), ASL5 (lime green). The six residues along these loops known to anchor two Zn(II) ions (shown as gray spheres) in the active site are labelled and shown as sticks (H120, H122, D124, H189, C208, H250). Located on ASL1 and shown as sticks, F70 is important for substrate binding and recognition. An important target for covalent inhibitors, K211 is shown as sticks along ASL4. The two residues mutated in the clinical variants used for this study are shown as sticks as well: M154 (red) and A233 (green).

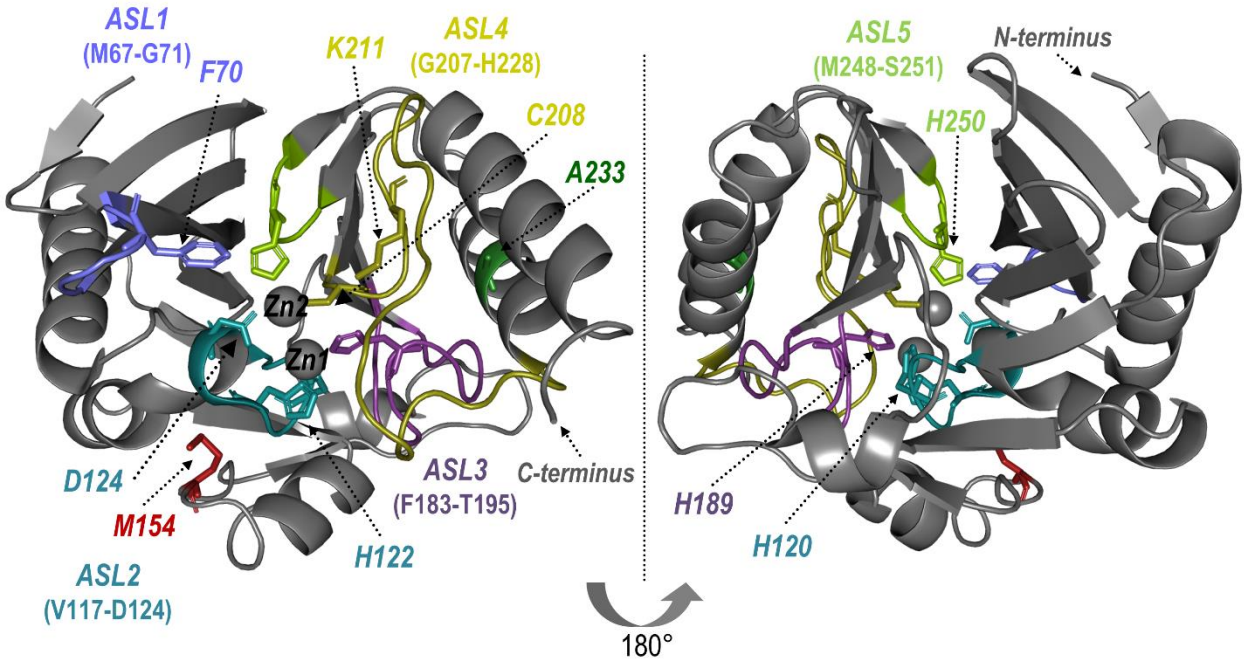

Figure S4. Time-dependent Inactivation of NDM-1 by **1**. Purified NDM-1 (0.5 μM) was incubated with inhibitor (**1**) (10 μM) in the presence of $ZnSO_4$ (10 μM), HEPES (50 mM), DMSO (1% v/v) at pH 7.0, 25 °C. At various timepoints, aliquots were diluted 25-fold into a reaction mixture containing chromacef (20 μM), $ZnSO_4$ (10 μM), and HEPES (50 mM) at pH 7.0, 25 °C, and the activity monitored by UV-vis as described previously.[1] Values for activity remaining were calculated as a percent of the uninhibited activity at each timepoint determined using a parallel incubation in which inhibitor was omitted (but 1% DMSO cosolvent included for consistency). The fit shown is to a single exponential decay to yield k_{obs} 0.035 ± 0.003 min^{-1} for this concentration of (**1**).

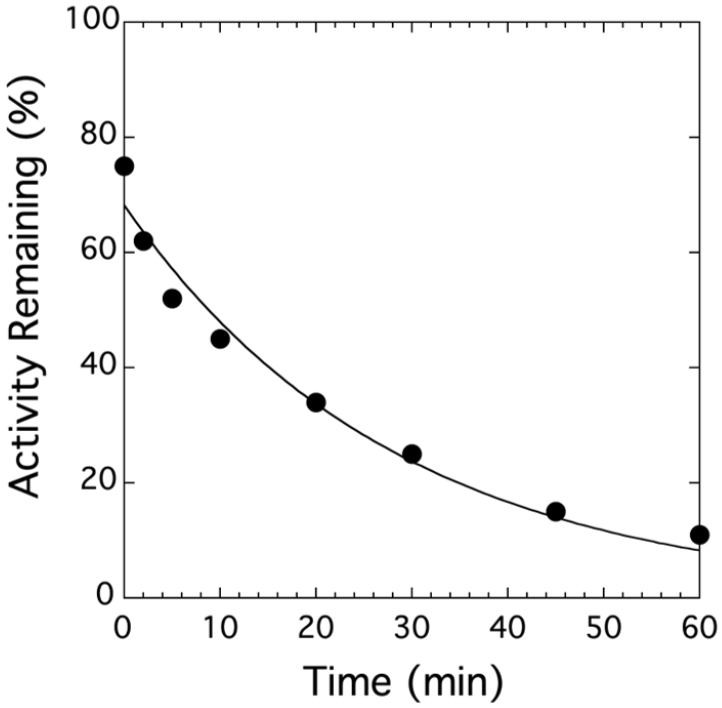

Figure S5. ESI mass spectra of (-) NDM-1 and (+) NDM-1 reacted with inhibitor (**1**) at various inhibitor:protein ratios (1:1, 5:1, 100:1) sprayed under (A) denaturing or (B) native conditions. Deconvolution reveals that up to three inhibitors can bind to NDM-1 and, under native conditions, attachment of the inhibitor does not displace the Zn(II) ions. Open circles in (B) denote uninhibited NDM-1 in the reacted sample. Reported mass accuracies (ppm) account for mass shifts due to the covalent inhibitor or Zn(II) cofactors.

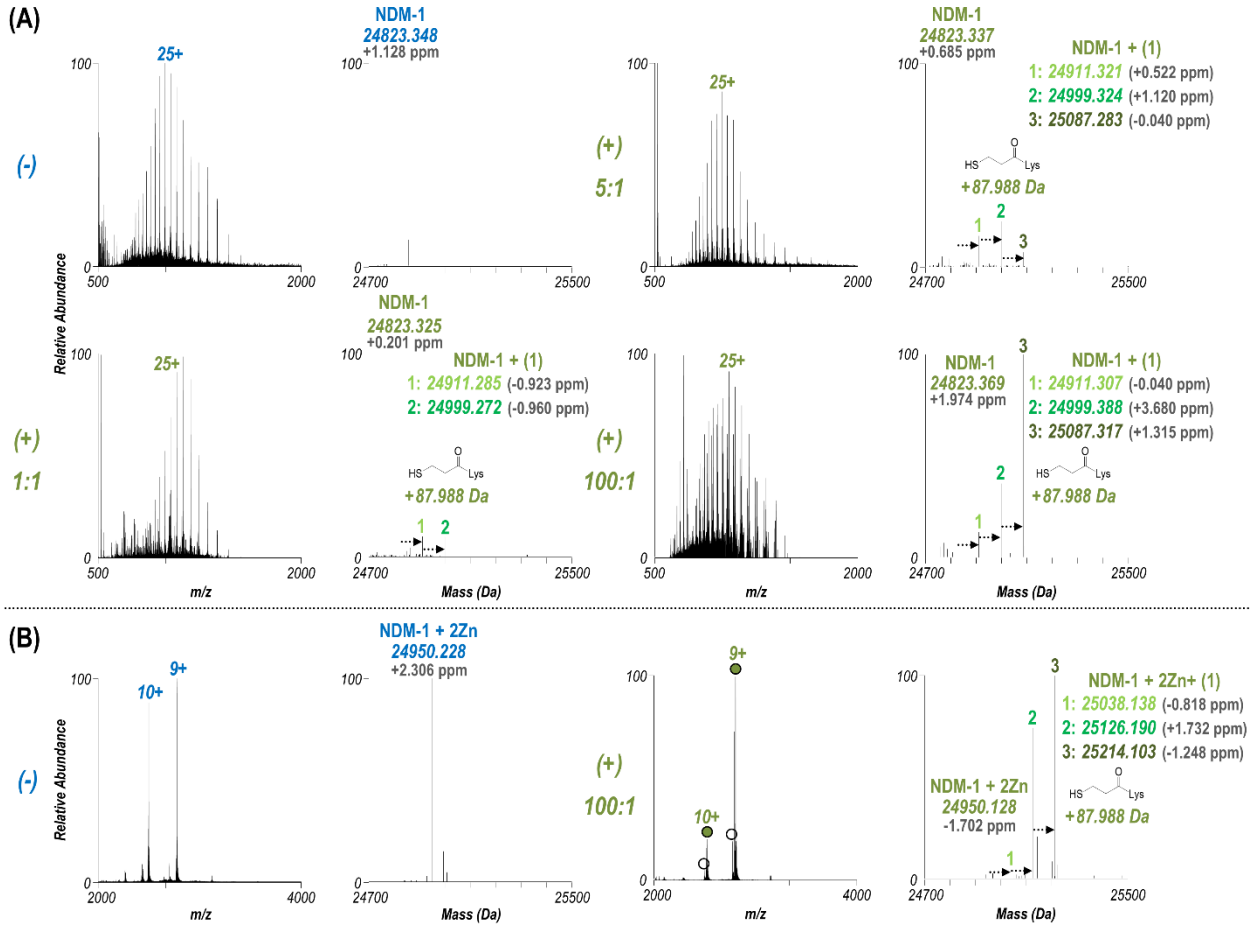

Figure S6. (A) HCD and (B) UVPD MS/MS spectra resulting from activation of the 25+ charge state of (-) NDM-1 or (+) NDM-1 covalently bound to one, two, or three of inhibitor (**1**). Abundant fragment ions are labelled for the uninhibited sample. Mass shifts of +88 Da in one of the most abundant fragment ions (y_{100}^{11+}) in both the HCD and UVPD spectra due to sequential addition of inhibitor (**1**) can be observed and is denoted by ♦.

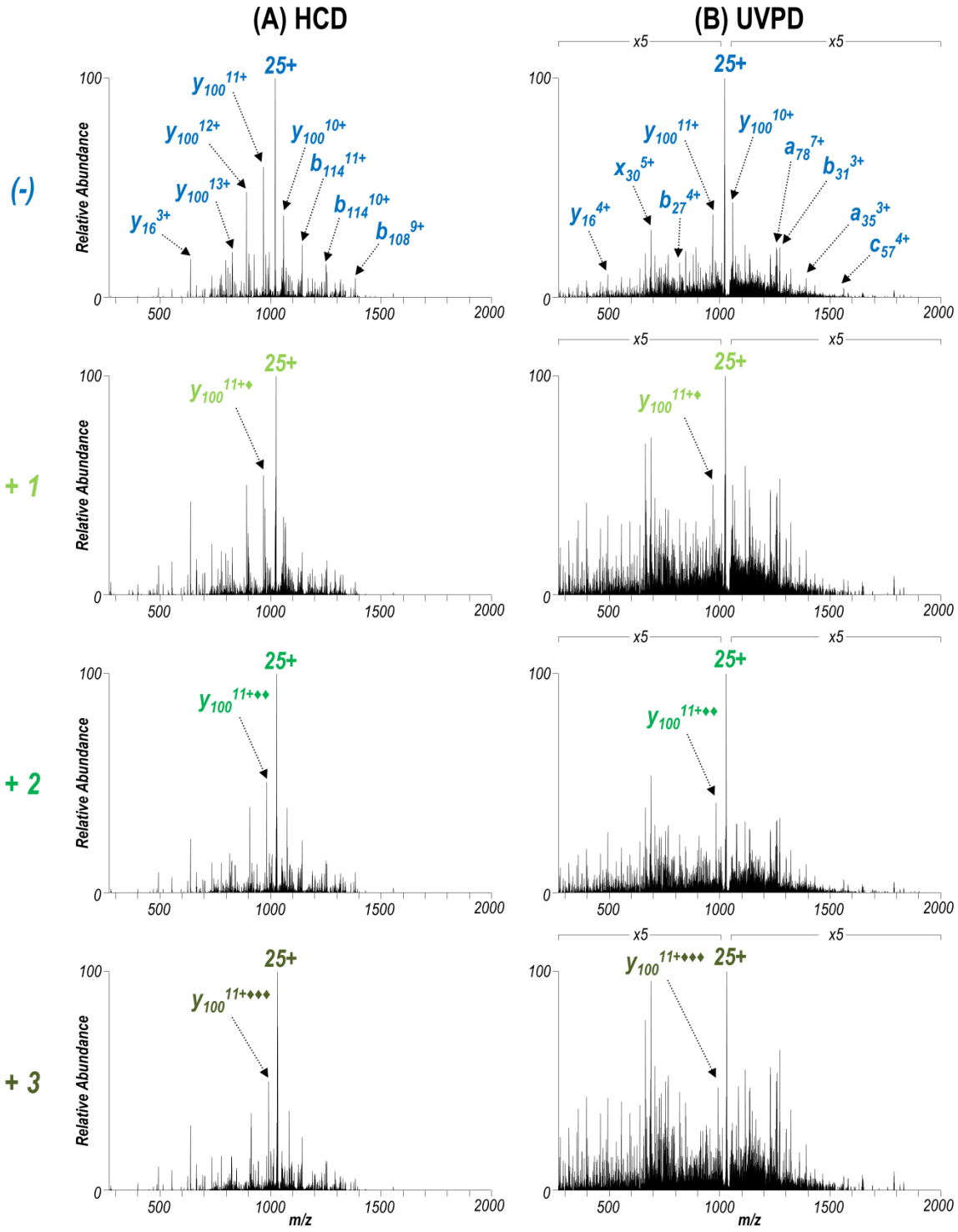

Figure S7. Deconvoluted (A) HCD and (B) UVPD spectra produced by activation of (-) NDM-1 or (+) NDM-1 covalently bound to one, two, or three of inhibitor (**1**). The corresponding MS/MS spectra are shown in Figure S6. Surviving precursor is labelled with a filled circle. Sequence coverage maps of identified fragment ions are shown with corresponding sequence coverage values. Static modifications of +88 Da were added to highlighted Lys residues. UVPD allowed complete localization of up to three inhibitor (**1**).

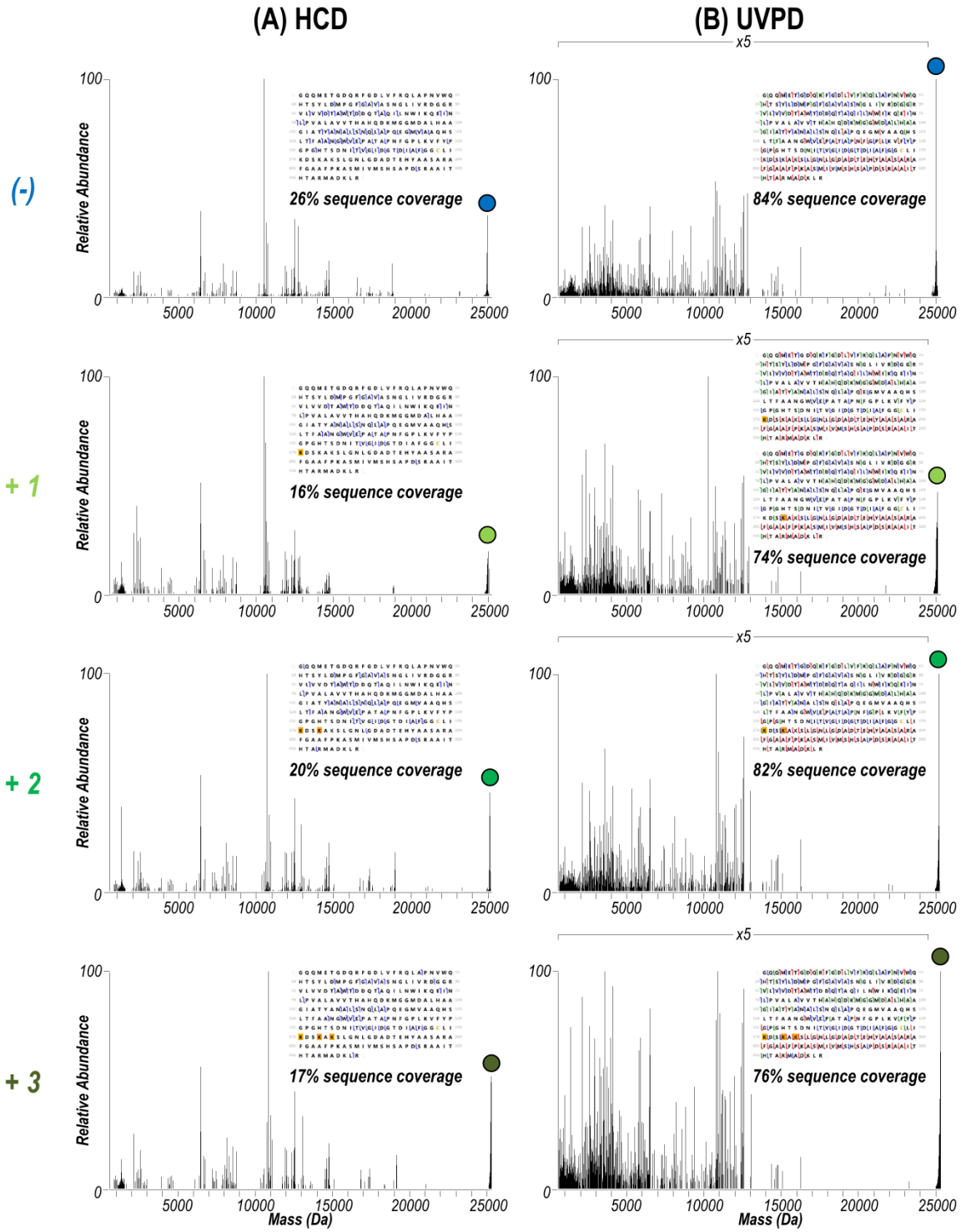

Figure S8. Native ESI mass spectra of (-) NDM-1 and (+) NDM-1 reacted with inhibitor (**2**) with observed charge states labelled (8+, 9+). Unreacted NDM was observed in the reacted sample (open circles). The right panel shows the corresponding deconvoluted spectra. Both Zn(II) cofactors were retained after covalent attachment of inhibitor (**2**). Mass shifts for the inhibitor and Zn(II) cofactors are accounted for when calculating accuracies (ppm).

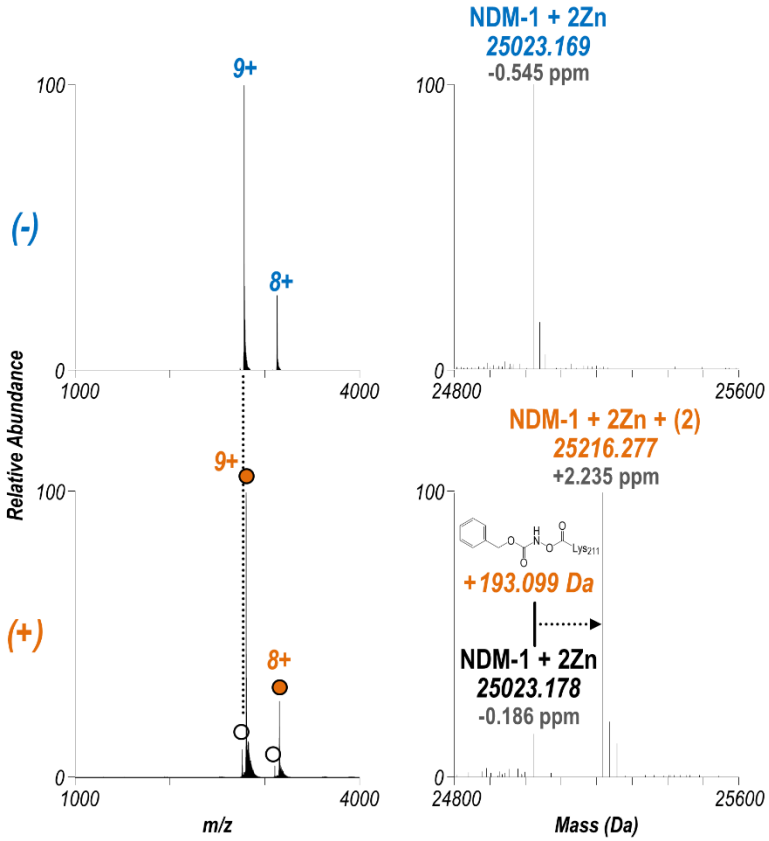

Figure S9. (A) UVPD MS/MS spectra of the 9+ charge state of (-) NDM-1 and (+) NDM-1 bound covalently to inhibitor (**2**). Corresponding deconvoluted UVPD spectra are shown in (B) with the precursor identified by a filled circle. Several abundant fragment ions are labelled in which the ♦ denotes a mass shift corresponding to inhibitor (**2**). (C) Apo and holo (Zn-bound) fragment ions produced by UVPD are mapped along the protein sequence. A +193 Da static modification at K211 (highlighted yellow) was considered to localize covalent attachment of the inhibitor.

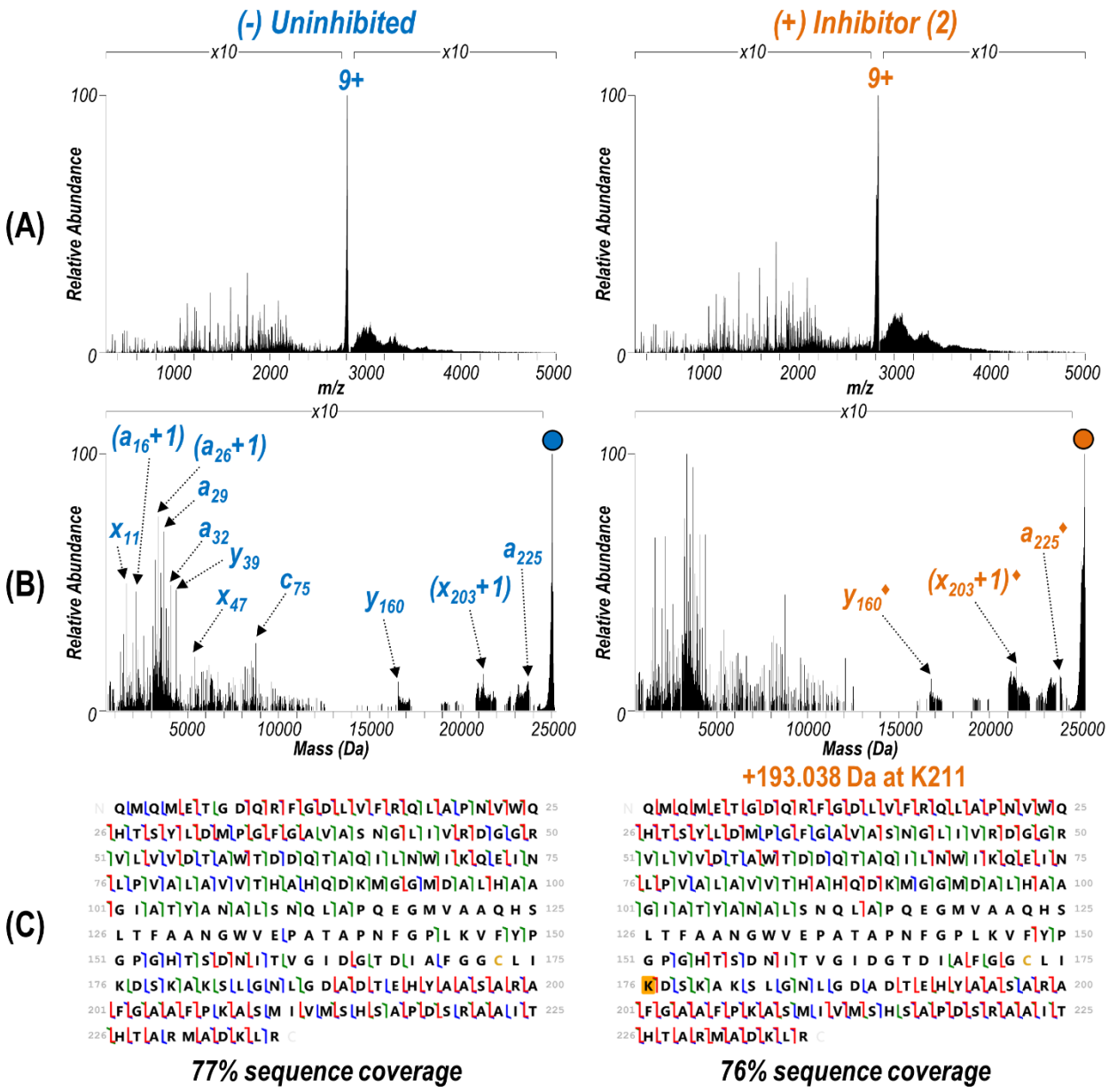

Figure S10. (A) Intensities (summed and normalized to the TIC) of identified UVPD fragment ions plotted per residue for uninhibited NDM-1 (blue) and NDM-1 bound to inhibitor (**2**) (orange). Subtracting the values for uninhibited NDM-1 from the corresponding values for inhibitor-bound NDM-1 yields the difference plot in Figure 3. (B) Heatmap representing the log of the values in (A) shown along the linear protein sequence.

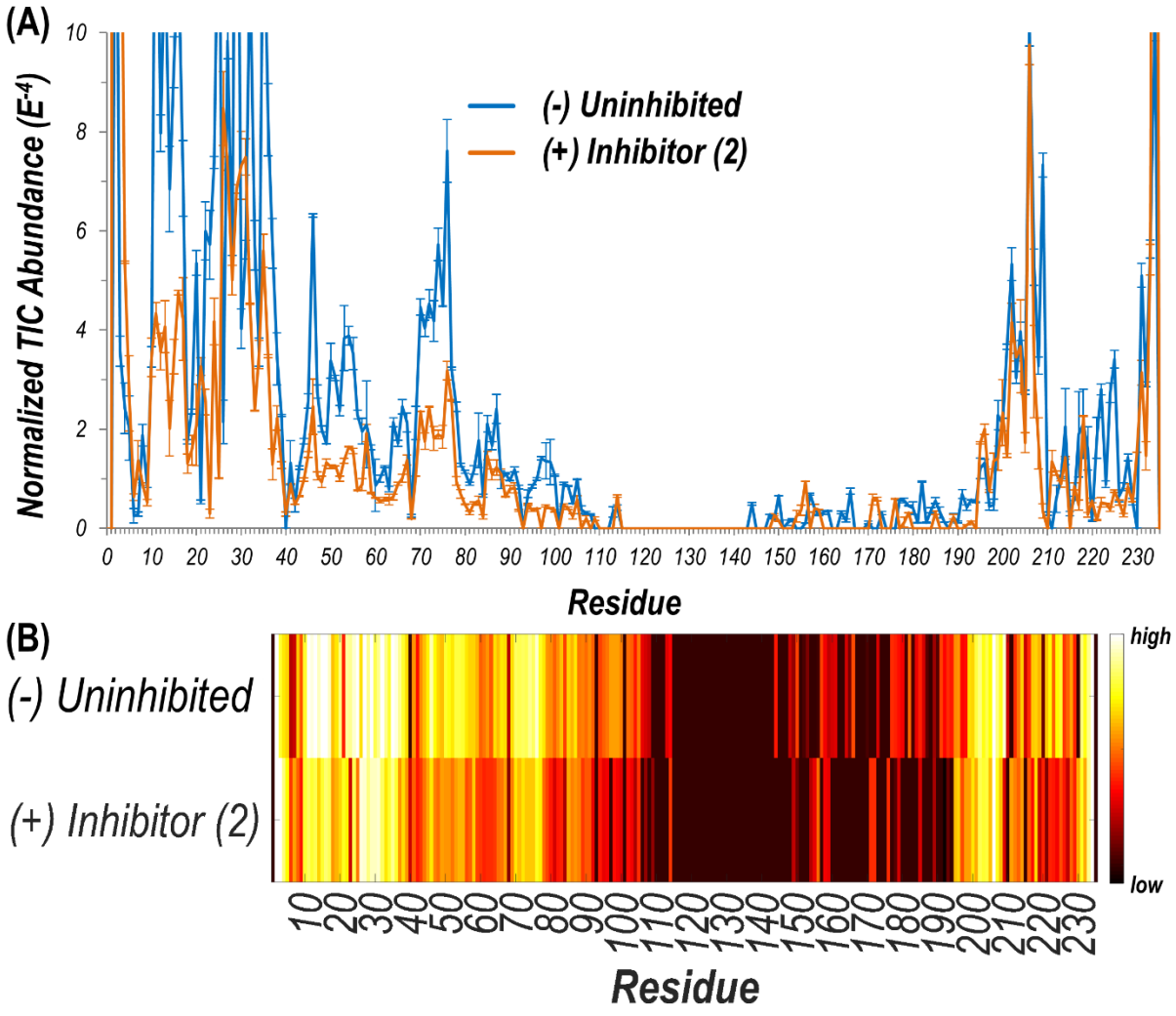

Figure S11. ESI mass spectra sprayed under (A) denaturing and (B) native conditions of (-) NDM-1 and (+) NDM-1 reacted with ebselen. The charge states observed in (B) are labelled (uninhibited: 8+ – 11+; reacted: 8+ – 18+). Corresponding deconvoluted spectra are shown to the right. Addition of ebselen causes loss of one of the Zn(II) ions as evidenced in (B). Accuracies (ppm) are calculated accounting for mass shifts due to covalent attachment of the inhibitor or non-covalent retention of metal cofactors.

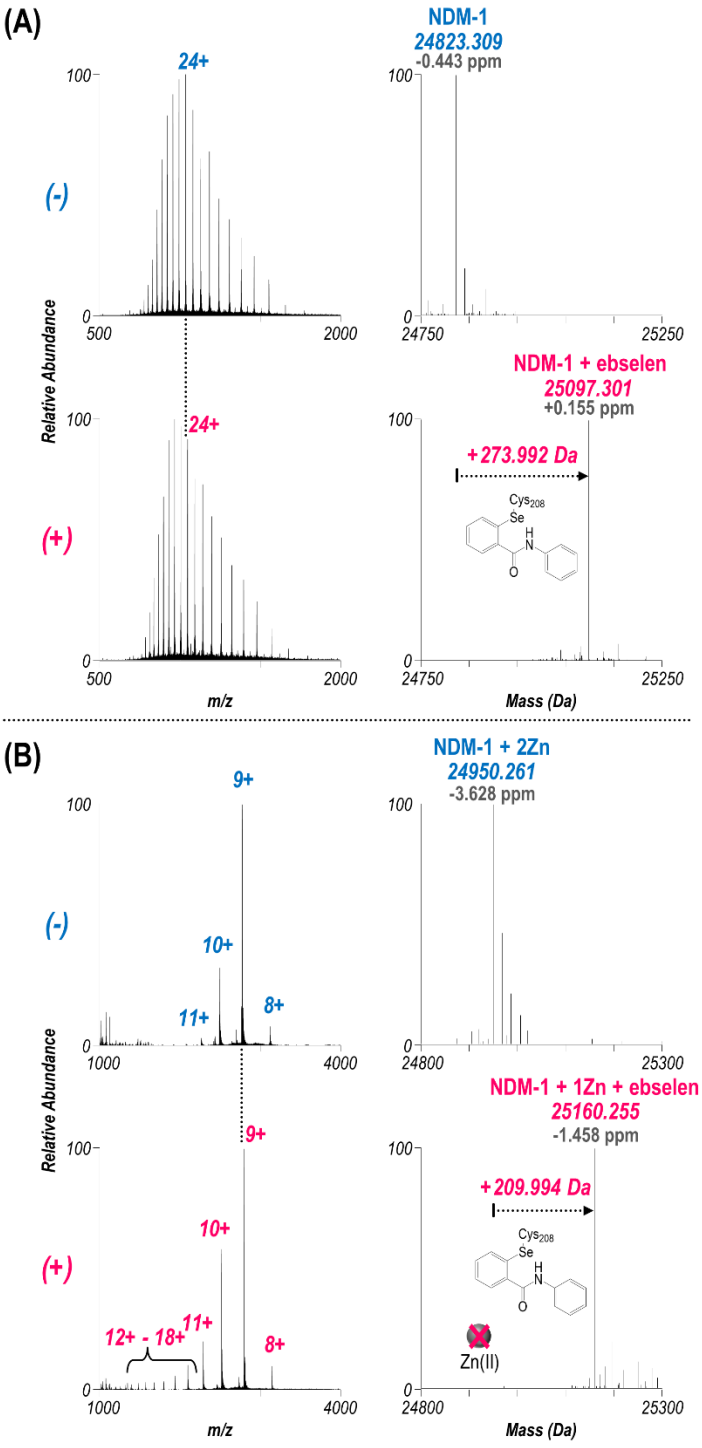

Figure S12. (A) UVPD MS/MS spectra collected while spraying under denaturing conditions of the 24+ charge state of (-) NDM-1 and (+) NDM-1 bound covalently to ebselen. The corresponding deconvoluted spectra are shown in (B) with the precursor identified with a filled circle and several abundant fragment ions labelled. Fragment ions labelled with a ♦ are mass shifted +273 Da and contain the inhibitor. (C) Sequence coverage maps of identified fragment ions resulting from UVPD. For the reacted sample, a static modification was added at the highlighted Cys (C208) allowing localization of the inhibitor to that residue.

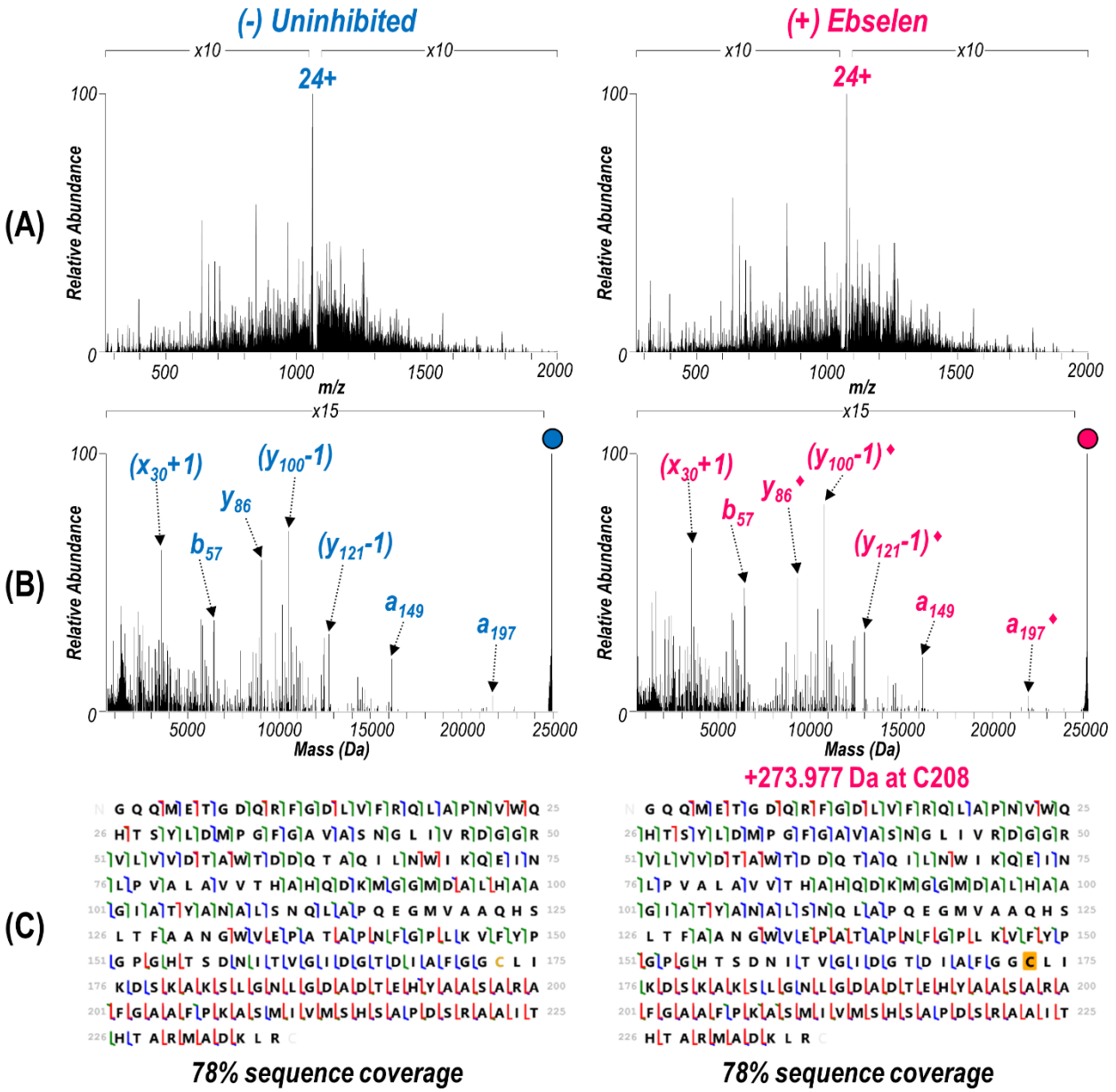

Figure S13. (A) MS/MS spectra produced by UV photoactivation of the 9+ charge state of (-) NDM-1 and (+) NDM-1 bound covalently to ebselen sprayed under native conditions. (B) Deconvoluted UVPD spectra corresponding to the MS/MS spectra in (A). The precursor is denoted by a filled circle. The inset (*m/z* 9300-9500) highlights a fragment ion observed in both the apo and holo (Zn-bound; indicated by an *) forms for the uninhibited sample but only in the apo form for the inhibitor bound species. (C) Sequence coverage maps accounting for identified apo and holo (Zn-bound) fragment ions resulting from UVPD. Searching with a +273 Da static modification at C208 (highlighted yellow) allows localization of the inhibitor to that residue.

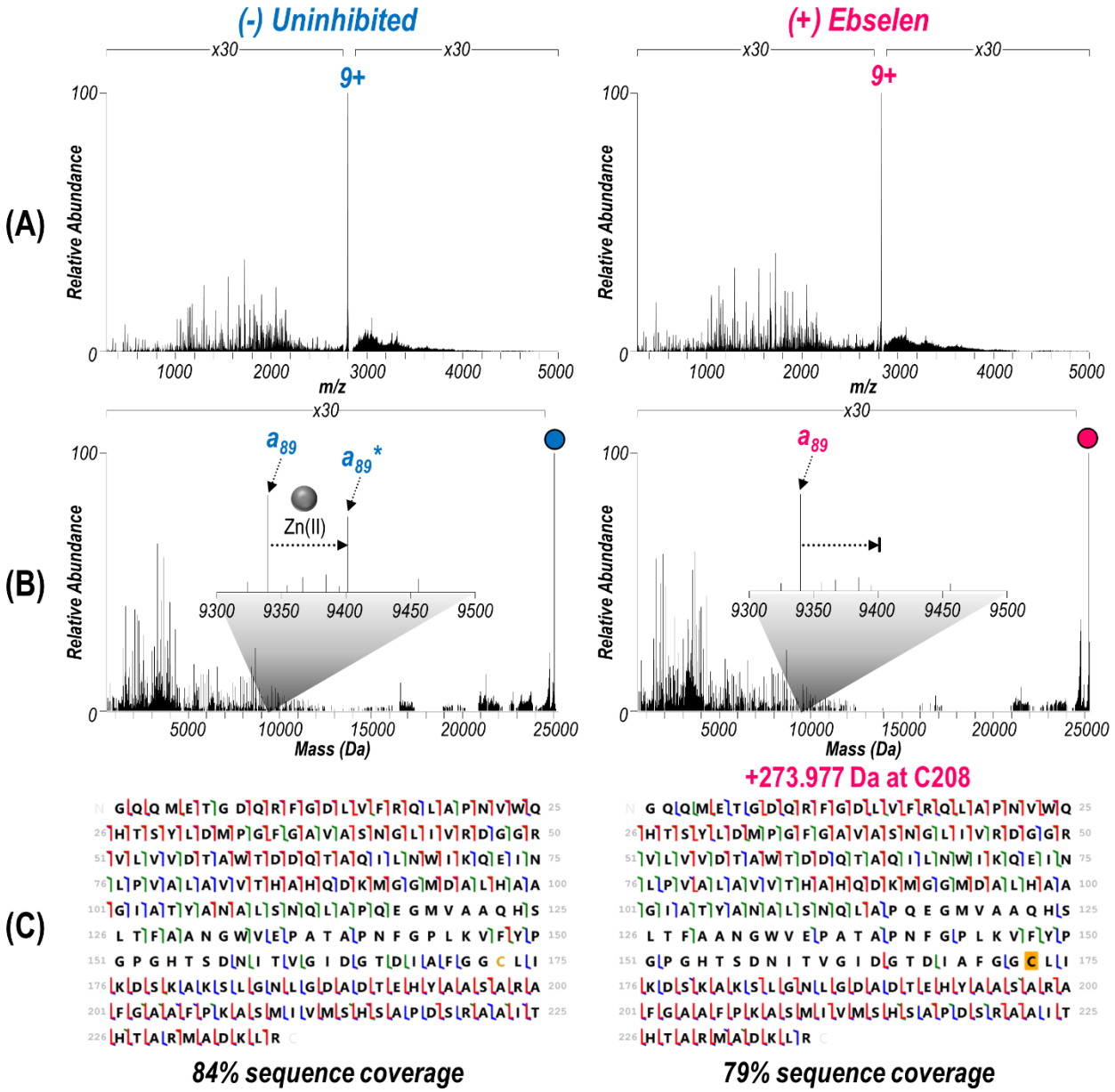

Figure S14. Crystal structure map (PDB ID: 3SPU) of (A) singly and (B) doubly Zn(II) bound holo ions for an unreacted NDM-1 sample. A corresponding combined map is shown in Figure 4. Residue color indicates whether the holo fragment ion is N-terminal (blue), C-terminal (red), or bi-directional (green). Ions were identified from the UVPD spectra shown in Figure S13. Bi-directional fragmentation is defined as complementary N- and C-terminal holo ions resulting from cleavage at the same backbone position. The six residues known to bind the cofactors are represented as sticks.

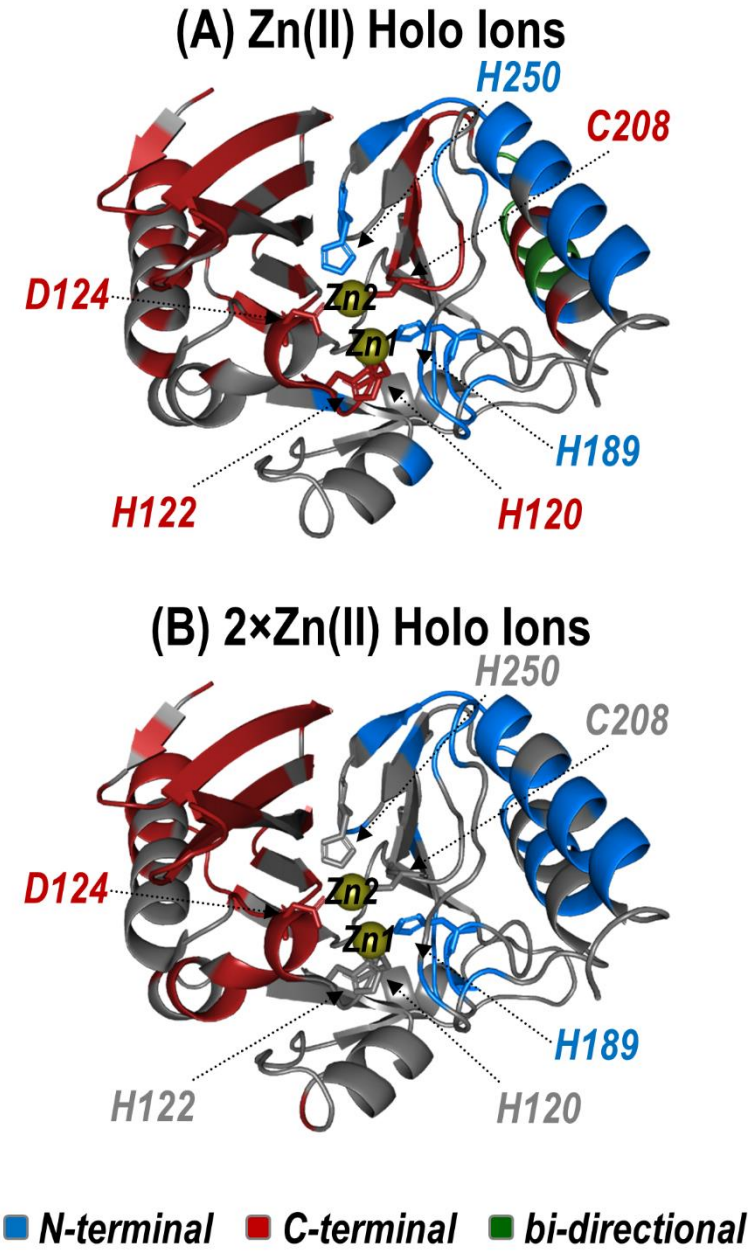

Figure S15. (A) Plot per residue of the abundances of identified fragment ions summed and normalized to the TIC for uninhibited NDM-1 (blue) and ebselen-bound NDM-1 (pink). The difference plot in Figure S16 was created by subtraction of the values for unihibited NDM-1 from the corresponding values for ebselen-bound NDM-1. (B) Log of the values in (A) shown as a linear heatmap along the sequence.

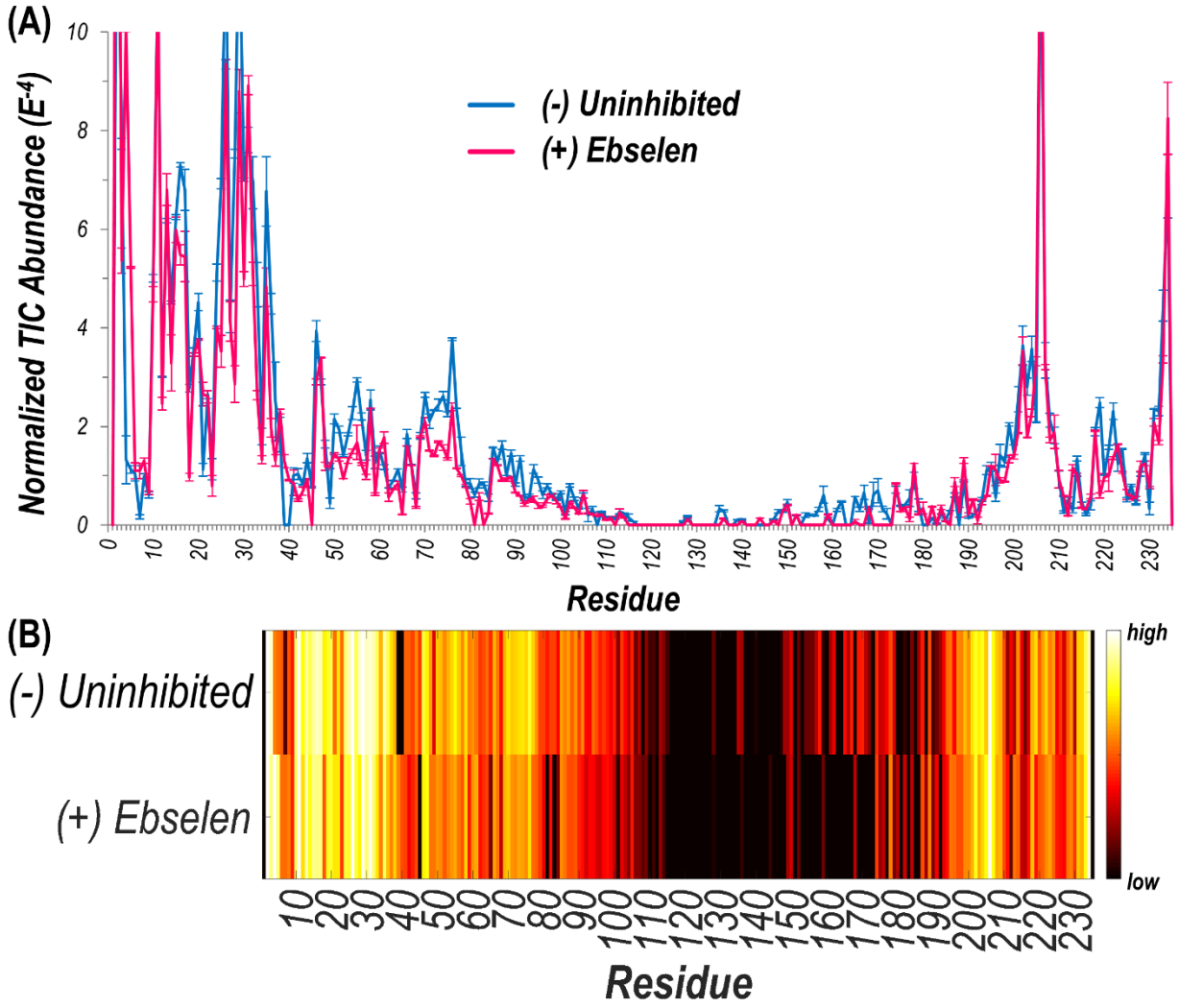

Figure S16. (A) Changes in abundances represented as a difference plot of apo and holo UVPD fragment ions between NDM-1 bound covalently to ebselen and an uninhibited sample resulting from subtraction of the UVPD fragmentation plots shown in Figure S15. ASL1 is outlined with a dashed slate line while the six residues known to bind the Zn(II) cofactors are highlighted with dashed black lines. (B) Linear and (C) crystal structure (PDB ID: 3SPU) heatmap representations are shown. Suppression in backbone cleavage efficiency of the inhibitor-bound species compared to the uninhibited is indicated by blue regions while enhancement is represented by red regions. In (C), ASL1 is displayed as spheres and the Zn(II)-binding residues are shown as sticks. The inhibitor attaches covalently at C208.

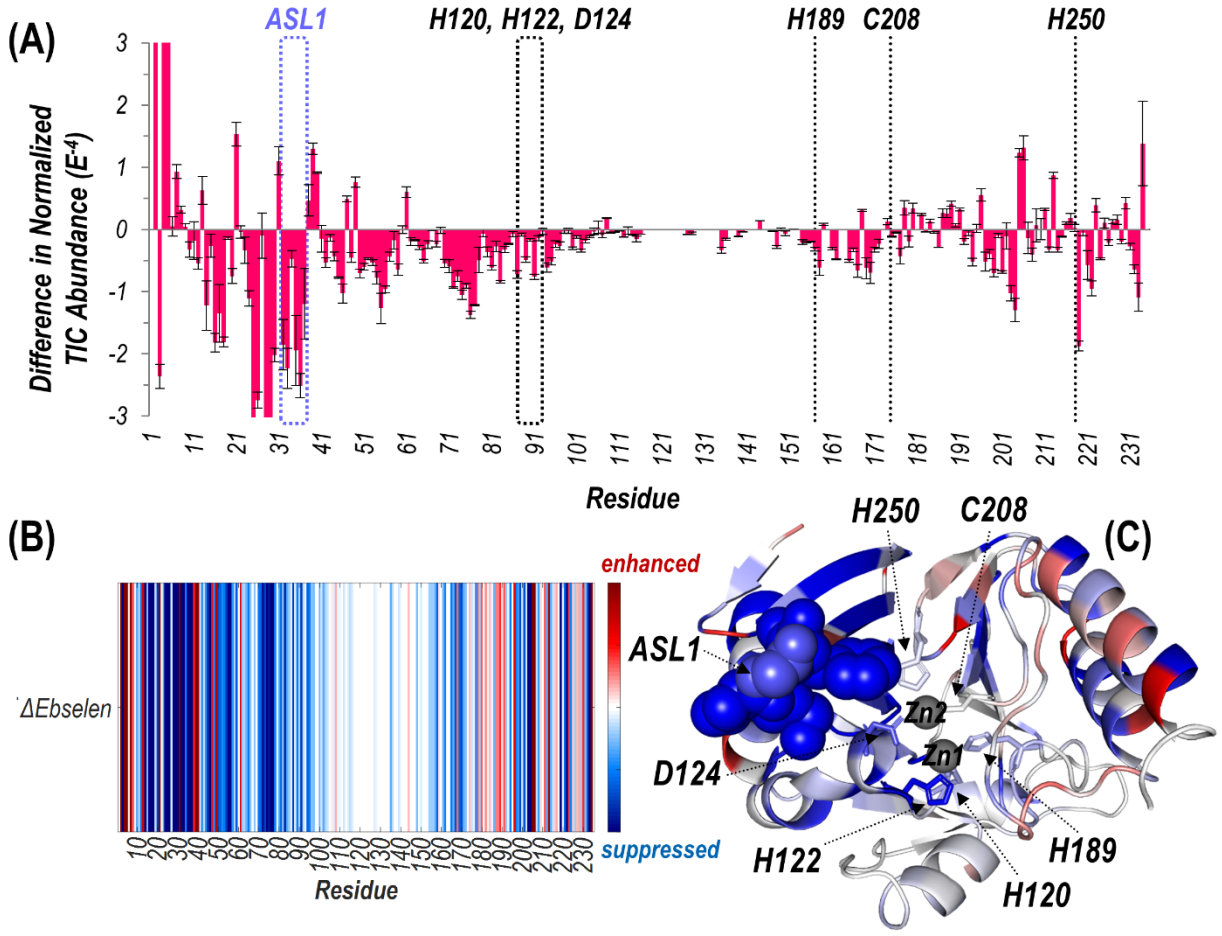

Figure S17. (1) Native ESI mass spectra of (A) NDM-1, (B) NDM-4, (C) NDM-6, and (D) NDM-15 with observed charge states labelled (9+, 10+, 11+). Corresponding deconvoluted spectra are shown in (2). Observed masses were +126 Da from theoretical masses based on protein sequence indicating that two Zn(II) ions are retained. Accuracies (ppm) are calculated accounting for the mass shift of the metal cofactors.

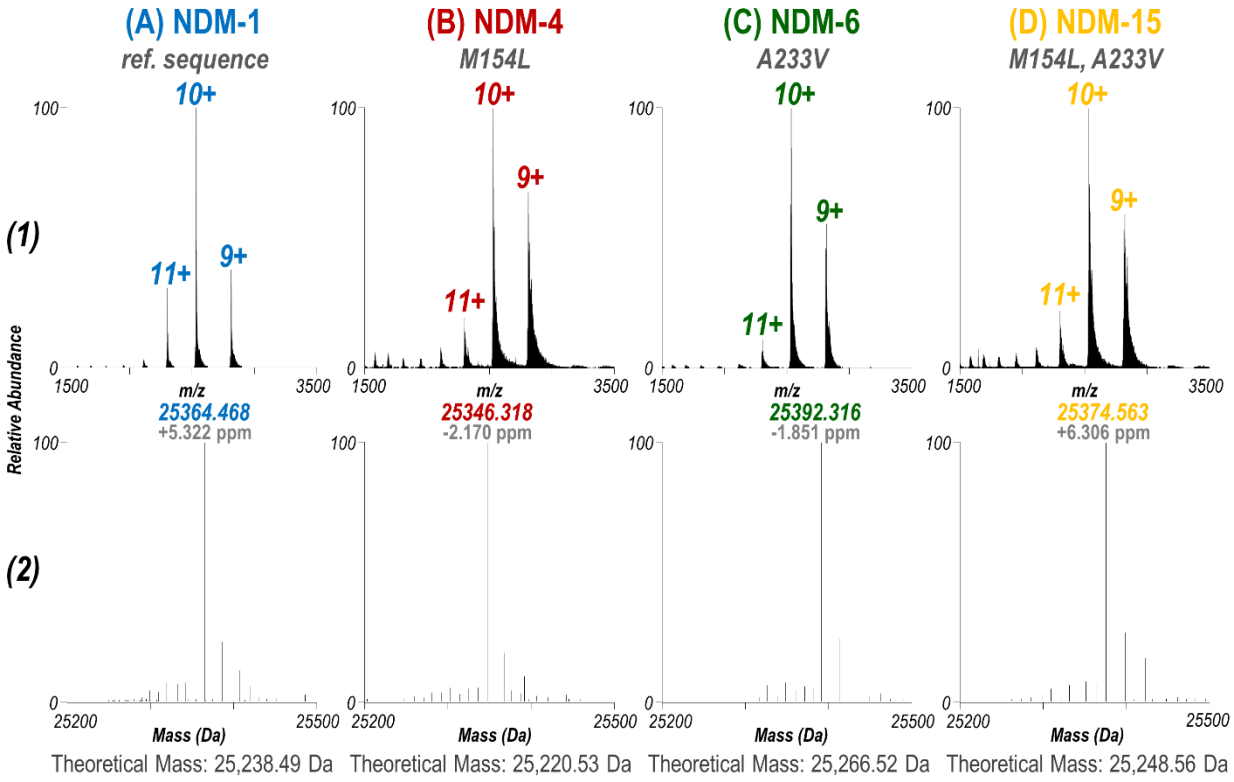

Figure S18. UVPD MS/MS spectra (one pulse at 3 mJ) of the 9+ charge state of NDM clinical variants: (A) NDM-1, (B) NDM-4, (C) NDM-6, and (D) NDM-15. In panel (A) several of the most abundant fragment ions are labelled. Surviving precursor is identified with a filled circle.

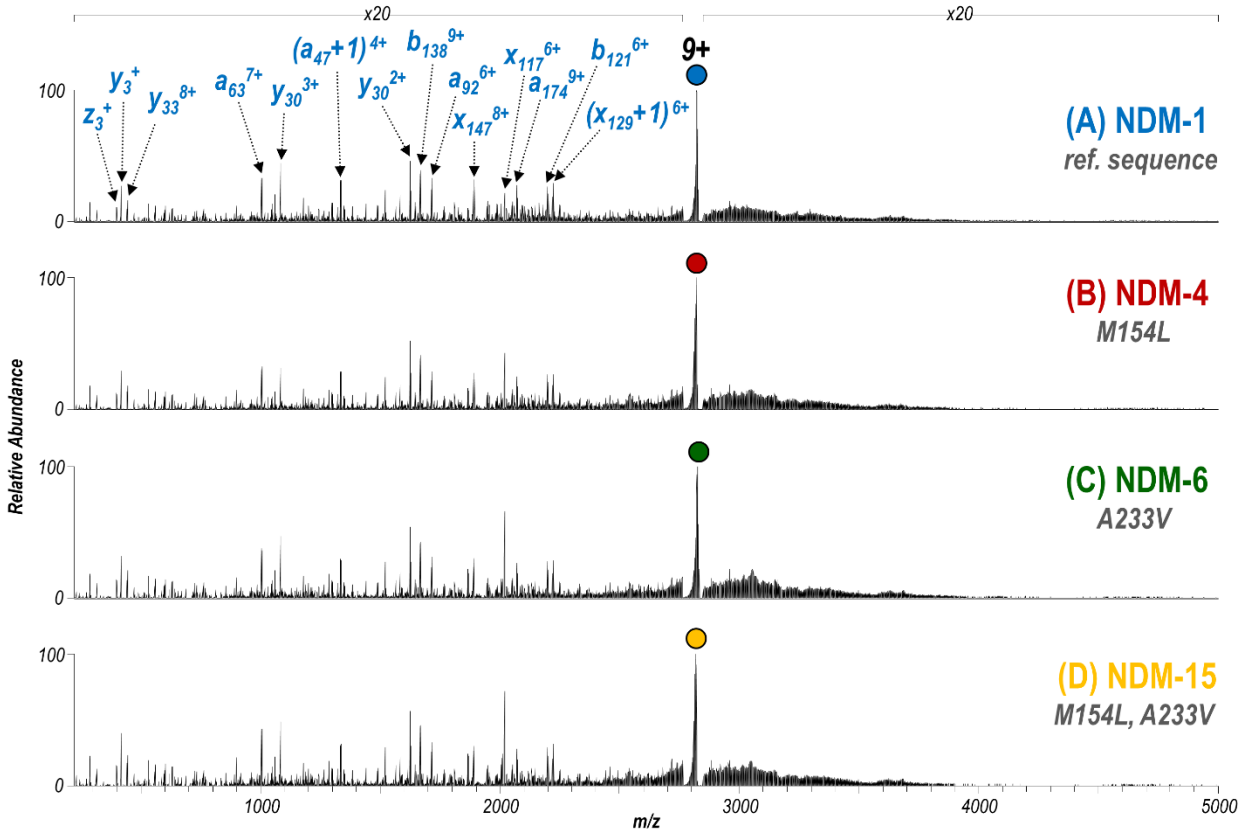

Figure S19. (A-D) Deconvoluted UVPD mass spectra of the corresponding spectra shown in Figure S18 for activation of the 9+ charge state of four clinical variants of NDM. The precursor is labelled with a filled circle. Sequence coverage maps and values of identified fragment ions are shown for each spectrum. These account for apo (Zn-free) and holo (Zn-bound) fragment ions. For the variants, the mutated residue(s) is highlighted in yellow.

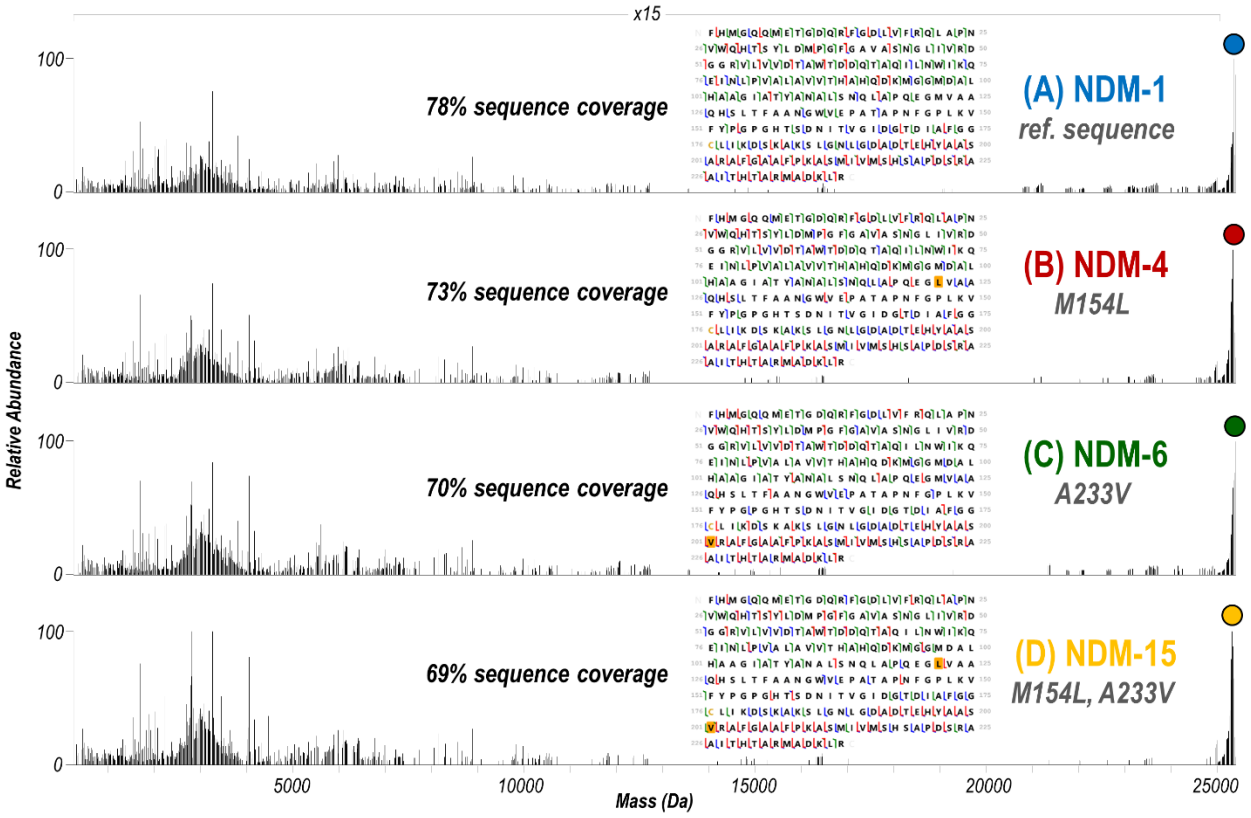

Figure S20. (A) Abundance of apo and holo fragment ions (summed and normalized to TIC) plotted per residue for NDM-1 (blue), NDM-4 (red), NDM-6 (green), and NDM-15 (yellow). Larger values indicate greater extents of backbone cleavages adjacent to the amino acid. Subtraction of the values for NDM-1 from the corresponding values for each of the variants was used to create the difference plots in Figure S21. (B) Linear heatmap of the log of the values in (A) shown along the sequence.

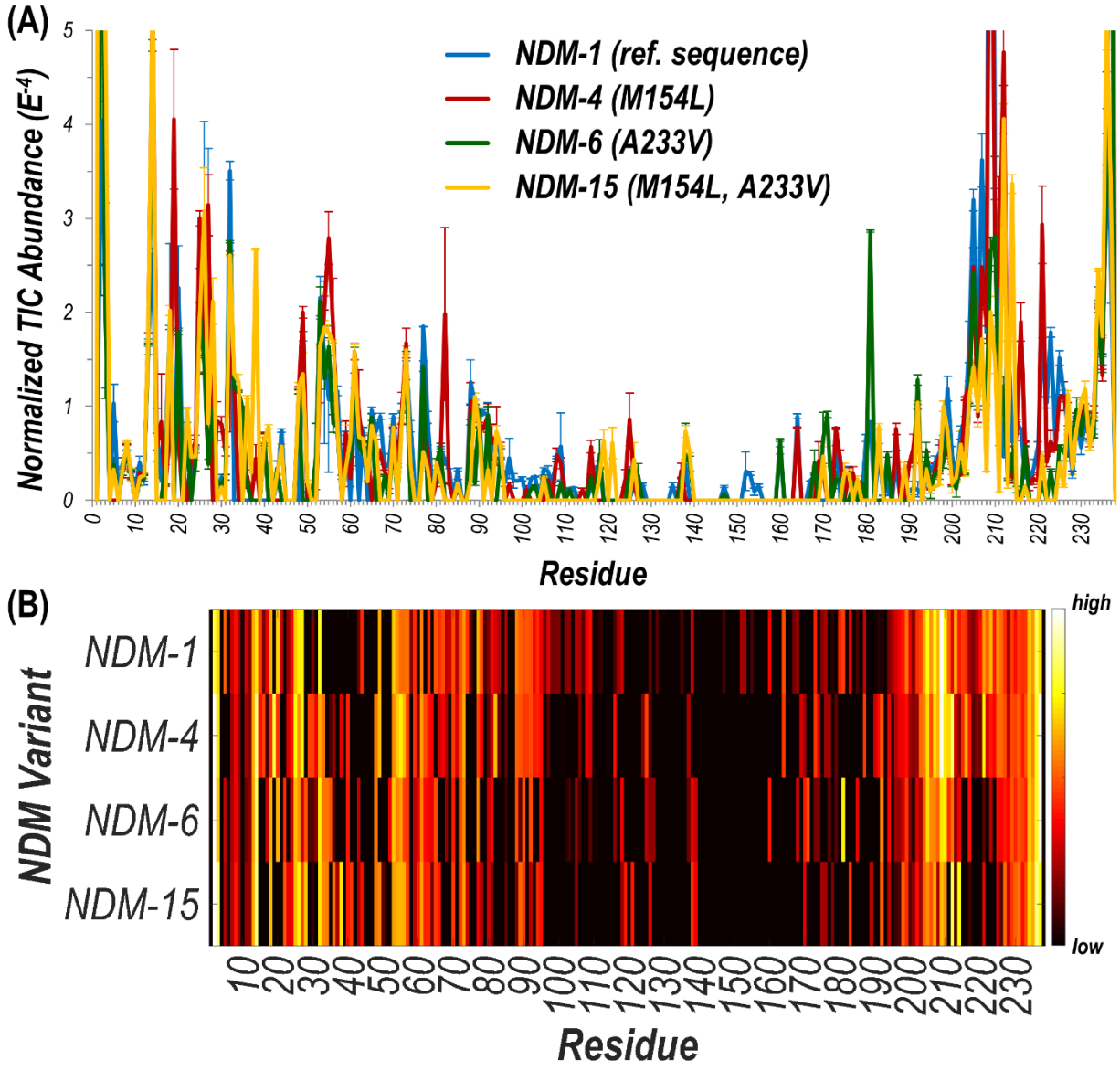

Figure S21. (A-C) Changes in the summed abundances of apo and Zn-bound holo fragment ions resulting from UVPD of three clinical variants of NDM compared to the reference NDM-1 sequence represented as difference plots. Values greater than zero indicate that the backbone cleavages are enhanced for the variant relative to NDM-1; values less than zero indicate that the backbone cleavages are suppressed for the variant. A plot of the summed backbone cleavage values used to create these graphs is shown in Figure S20. The six Zn-binding residues and two mutated residues (M154, A233) are indicated with dashed lines.

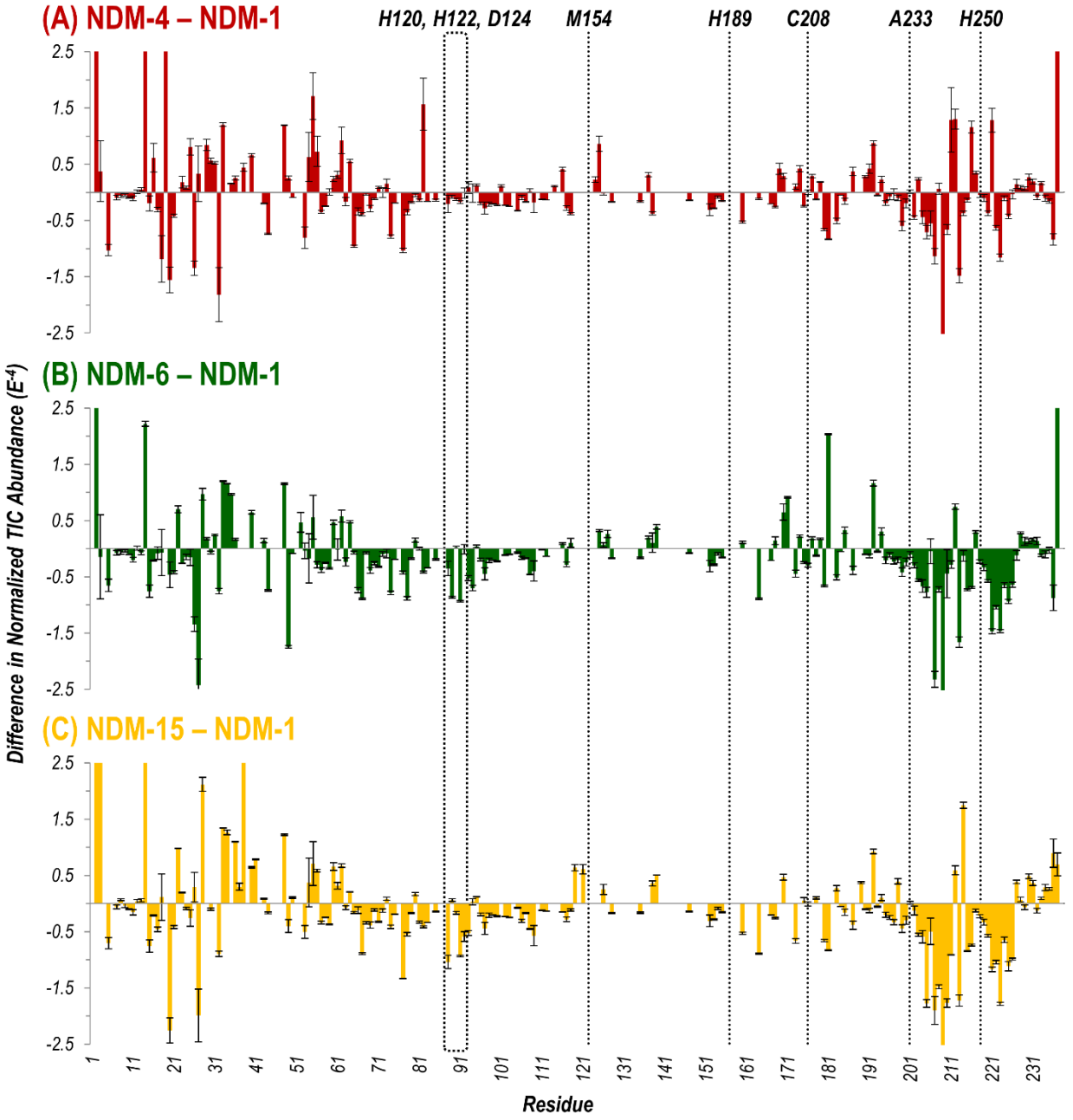

Figure S22. Changes in backbone cleavage efficiency during UVPD for three clinical variants of NDM (NDM-4, NDM-6, NDM-15) compared to the reference sequence (NDM-1) represented as heatmaps along the (A) linear sequence or (B-D) crystal structure (PDB ID: 3SPU) of NDM-1. Regions colored red indicate enhancement while blue regions denote suppression in UVPD cleavage efficiency of the variant compared to NDM-1, based on the difference plots shown in Figure 21. The mutated sites are shown as sticks (M154L, A233V). The six residues involved in binding the two Zn(II) ions represented as gray spheres are shown as sticks and labelled in (B).

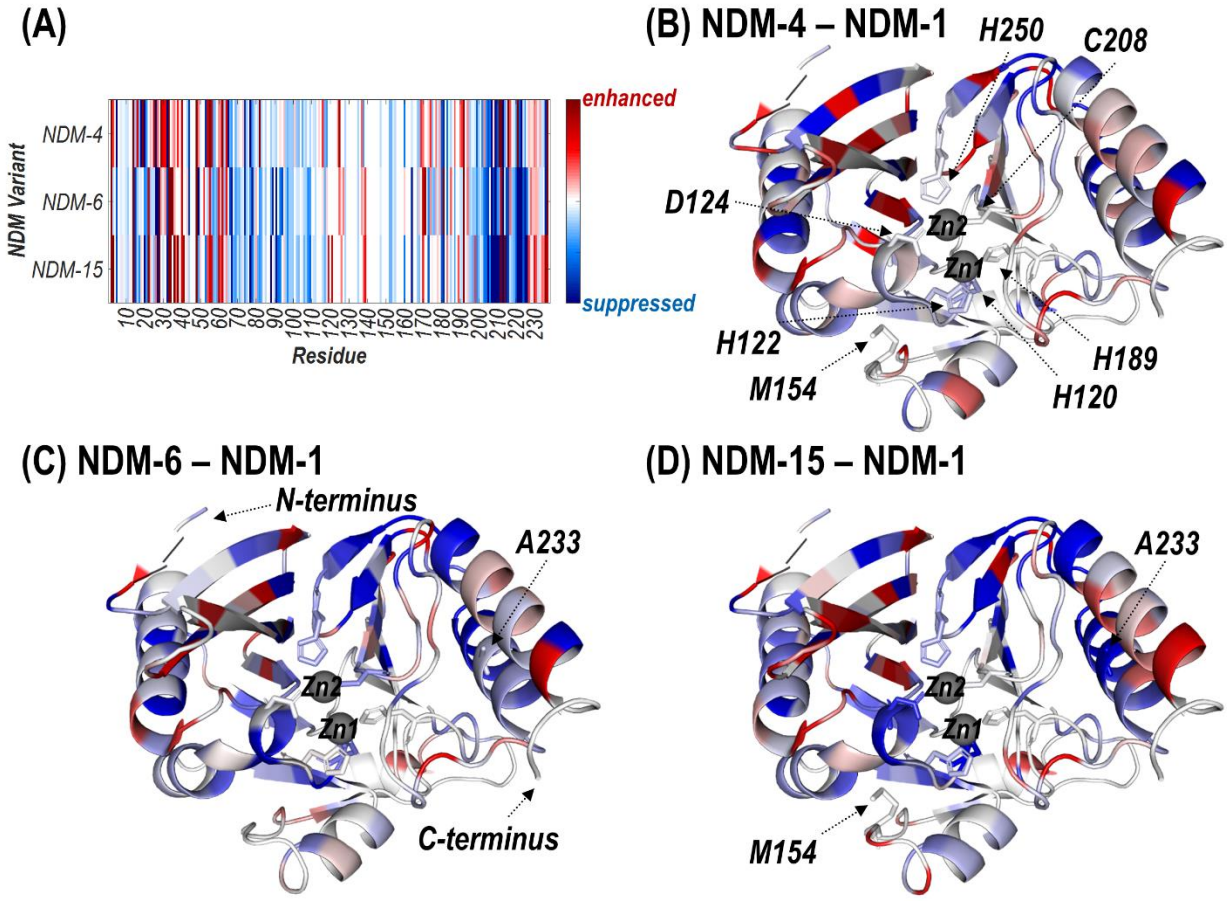

SUPPLEMENTAL INFORMATION REFERENCES

1 P. W. Thomas, M. Zheng, S. Wu, H. Guo, D. Liu, D. Xu and W. Fast, *Biochemistry*, 2011, **50**, 10102–10113.